Opacities in Astrophysics

Arthur N. Cox

Los Alamos Astrophysics

Group T-6

Los Alamos National Laboratory

Needs for Matter Opacities

- 1. Star Formation
- 2. Stellar Structure
- 3. Stellar Evolution
- 4. Stellar Pulsations
- 5. Stellar Explosions

OP Form for Calculating Stellar Opacities

Abundance Fractions

Hydrogen Abundance (X)	0.70
Metal Abundance (Z)	0.02

Metal Fractional Composition (default = solar)

Note: metal abudancies are re-normalised to the value of Z which has been set --- it is necessary to specify only the relative abundance for each metal.

C (Z=6)	0.2460	N (Z=7)	0.0647	O (Z=8)	0.5140
Ne (Z=10)	0.0815	Na (Z=11)	0.00148	Mg (Z=12)	0.02636
Al (Z=13)	0.00205	Si (Z=14)	0.0246	S (Z=16)	0.01125
Ar (Z=18)	0.0023	Ca (Z=20)	0.00159	Cr (Z=24)	0.000324
Mn (Z=25)	0.00017	Fe (Z=26)	0.02244	Ni (Z=28)	0.00123

OPAL MIXTURE COMPOSITION

type 2 number fractions

NORMALIZE RESET

Enhanced element 1: C (C-Si only)

Enhanced element 2: O (C-Si only)

Metallicity, Z: 0.0500 (0-0.2, input truncated to nearest 0.0001)

Symbol	Z	At. mass (a.u.)	My Fraction	Initial Fraction
H	1	1.00790		
He	2	4.00260		
C	6	12.01100	0.245518	0.245518
N	7	14.00670	0.064578	0.064578
O	8	15.99940	0.512966	0.512966
Ne	10	20.17900	0.083210	0.083210
Na	11	22.98977	0.001479	0.001479
Mg	12	24.30500	0.026308	0.026308
Al	13	26.98154	0.002042	0.002042
Si	14	28.08550	0.024552	0.024552
P	15	30.97376	0.000195	0.000195
S	16	32.06000	0.011222	0.011222
Cl	17	35.45300	0.000219	0.000219
Ar	18	39.94800	0.002291	0.002291
K	19	39.09830	0.000091	0.000091
Ca	20	40.08000	0.001586	0.001586
Ti	22	47.90000	0.000075	0.000075
Cr	24	51.99600	0.000329	0.000329
Mn	25	54.93800	0.000170	0.000170
Fe	26	55.84700	0.021877	0.021877
Ni	28	58.70000	0.001293	0.001293

These initial number fractions are set to the solar composition of Grevesse & Noels, 19

Los Alamos Astrophysics

Los Alamos TOPS Specification either number or weight fraction

Mix specification

Fraction by ◉ Number *or* ○ Mass.
Input format is ◉ Fraction, Element *or* ○ Fraction, Element, Isotopic weight.

In specifying a mix, the fraction represents relative numbers of atoms if the number fraction box is checked. If the mass fraction box is checked, the fraction represents relative masses of the specified elements. The fractions need not be normalized.

The element specification can be the atomic number, the chemical symbol (case insensitive) or the OPLIB matid. Thus aluminum can be specified as Al, al, 13, l13718 or n13718 (for the new denser photon energy grids).

If the "Fraction, Element, Isotope" box is checked, a specific isotopic weight must be entered for each element of the mixture. If this box is not checked, no isotopic weight should be entered, the Web Page will use the normal values.

User specified mixture. Up to 450 characters may be used for the mixture specification. User can choose to supply a name for the mixture, up to 15 characters.

1. al

Optional Mixture Name: [ ] (User supplied, maximum of 15 characters)

Effects of Spectral Lines on Los Alamos Opacities, Cox, 1965

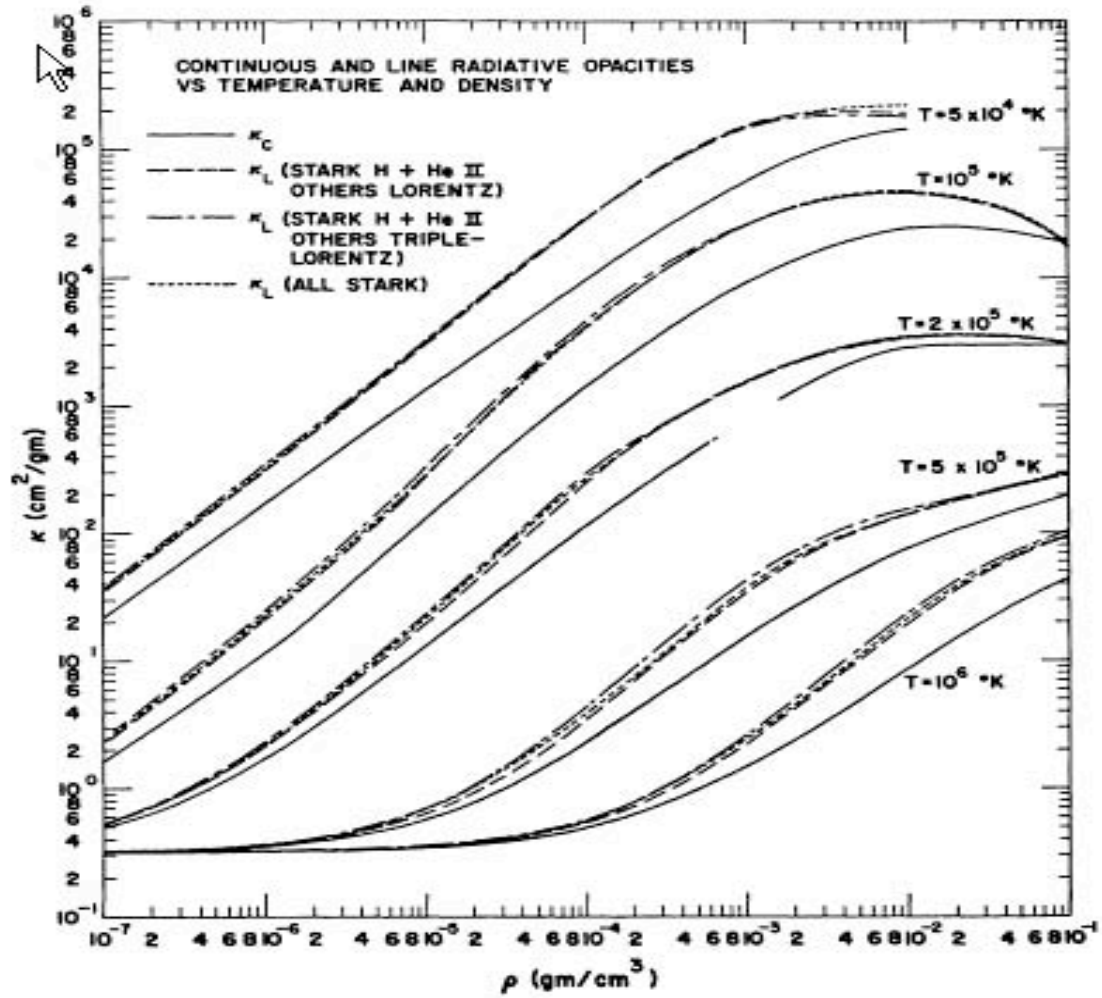

Cox and Tabor Astrophysical Journal Supplement 1976, ApJS,31, 271

Abstract

Radiative opacities for 40 mixtures of hydrogen, helium, and heavier elements are presented which represent the best large set of homogeneous data available for stellar structures. Smaller special tables of opacities are also calculated for specific applications in studies of stellar structure, evolution, and pulsation. Improvements in the computational methods include an increased iron abundance in the heavy-element composition, a better allowance for the ion continuum depression, and corrections in several bound-electron energy levels. It is noted that some of the opacities are not realistic because of zero hydrogen abundances or a lack of any possible molecules.

Updated OPAL Opacities
Iglesias, C.A. and Rogers. F.J.,1996, ApJ, 464, 943

Abstract

The reexamination of astrophysical opacities has eliminated gross discrepancies between a variety of observations and theoretical calculations; thus allowing for more detailed tests of stellar models. A number of such studies indicate that model results are sensitive to modest changes in the opacity. Consequently, it is desirable to update available opacity databases with recent improvements in physics, refinements of element abundance, and other such factors affecting the results.

Updated OPAL Rosseland mean opacities are presented. The new results have incorporated improvements in the physics and numerical procedures as well as corrections. The main opacity changes are increases of as much as 20% for Population I stars due to the explicit inclusion of 19 metals (compared to 12 metals in the earlier calculations) with the other modifications introducing opacity changes smaller than 10%. In addition, the temperature and density range covered by the updated opacity tables has been extended. As before, the tables allow accurate interpolation in density and temperature as well as hydrogen, helium, carbon, oxygen, and metal mass fractions. Although a specific metal composition is emphasized, opacity tables for different metal distributions can be made readily available. The updated opacities are compared to other work.

Subject headings: atomic data — atomic processes — stars: interiors

OPAL Solar Opacity Larger Than Old Los Alamos Opacity

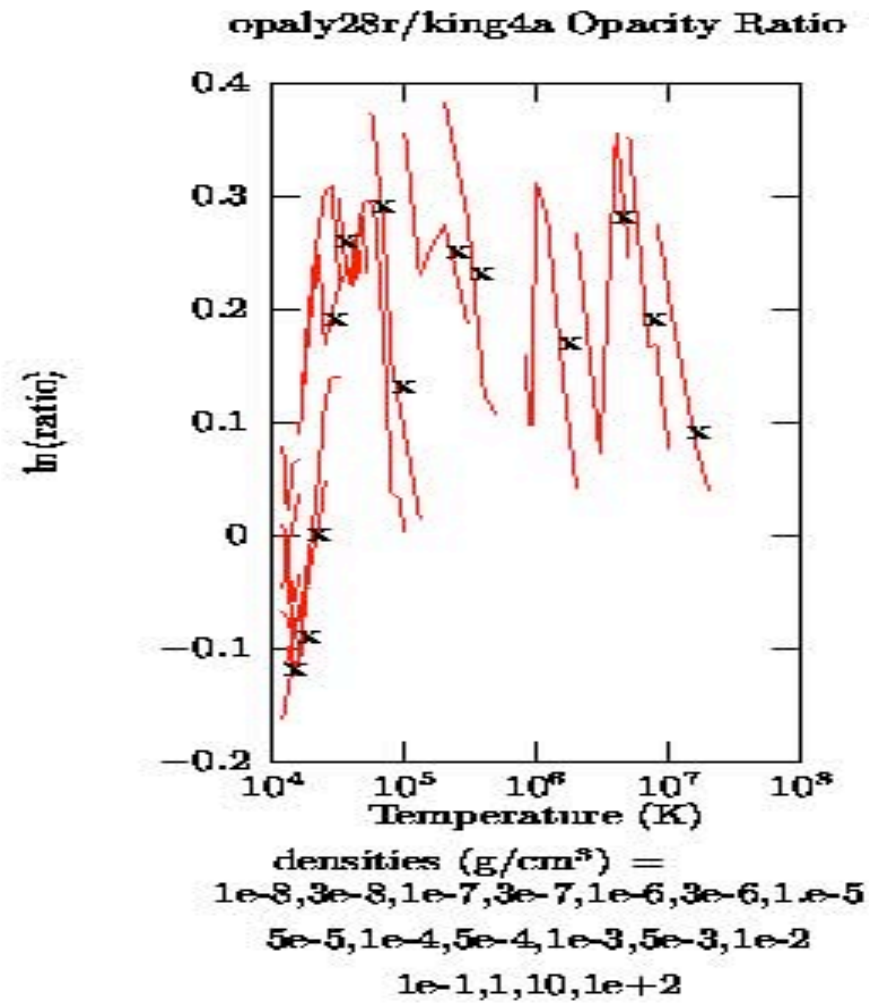

opaly28r Composition Cox-Tabor Z Composition

El	Z	A	N	X
H	1.0	1.00797E+00	9.07156E-01	7.00000E-01
He	2.0	4.00260E+00	9.13793E-02	2.80000E-01
C	6.0	1.20112E+01	2.84436E-04	2.61540E-03
N	7.0	1.40067E+01	8.01664E-05	8.59600E-04
O	8.0	1.59994E+01	6.36796E-04	7.79960E-03
Ne	10.0	2.01830E+01	3.58814E-04	5.54400E-03
Na	11.0	2.29898E+01	1.42048E-06	2.50000E-05
Mg	12.0	2.43120E+01	1.79456E-05	3.34000E-04
Al	13.0	2.69815E+01	1.19090E-06	2.46000E-05
Si	14.0	2.80860E+01	2.27711E-05	4.89600E-04
Ar	18.0	3.99480E+01	2.38377E-05	7.29000E-04
Fe	26.0	5.58470E+01	3.69376E-05	1.57920E-03

COMPOSITION OF Z FOR STANDARD MIXTURES

Element	Number Fraction	Mass Fraction
C.....	0.194250	0.13077
N.....	0.054747	0.04298
O.....	0.434873	0.38998
Ne.....	0.245034	0.27720
Na.....	0.000974	0.00125
Mg.....	0.012256	0.01670
Al.....	0.000810	0.00123
Si.....	0.015552	0.02448
Ar.....	0.016280	0.03645
Fe.....	0.025224	0.07896

Comparison of OPAL and OP Opacities for a Solar Mixture

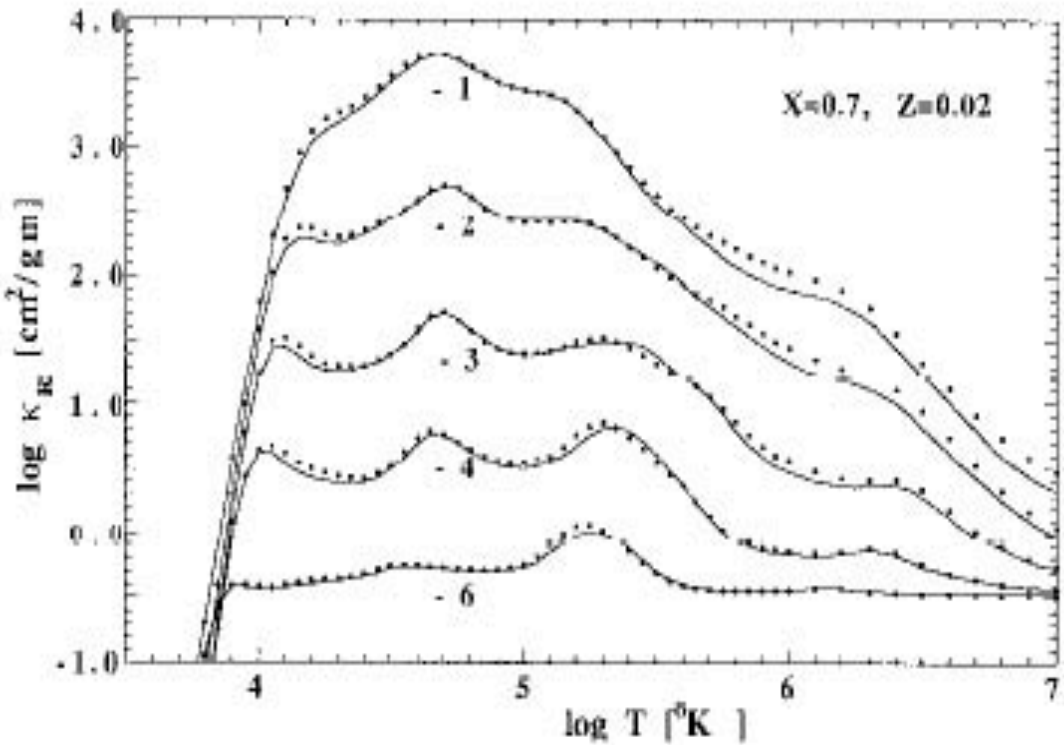

Figure 1. Comparison of OPAL (dots) and OP (solid lines) Rosseland mean opacities at constant values of log R for the element distribution used by Seaton *et al.* (1994) where X is the hydrogen mass fraction and Z is the metallicity.

The new OP opacities are only slightly larger than the OPAL opacities just below the solar convection zone.

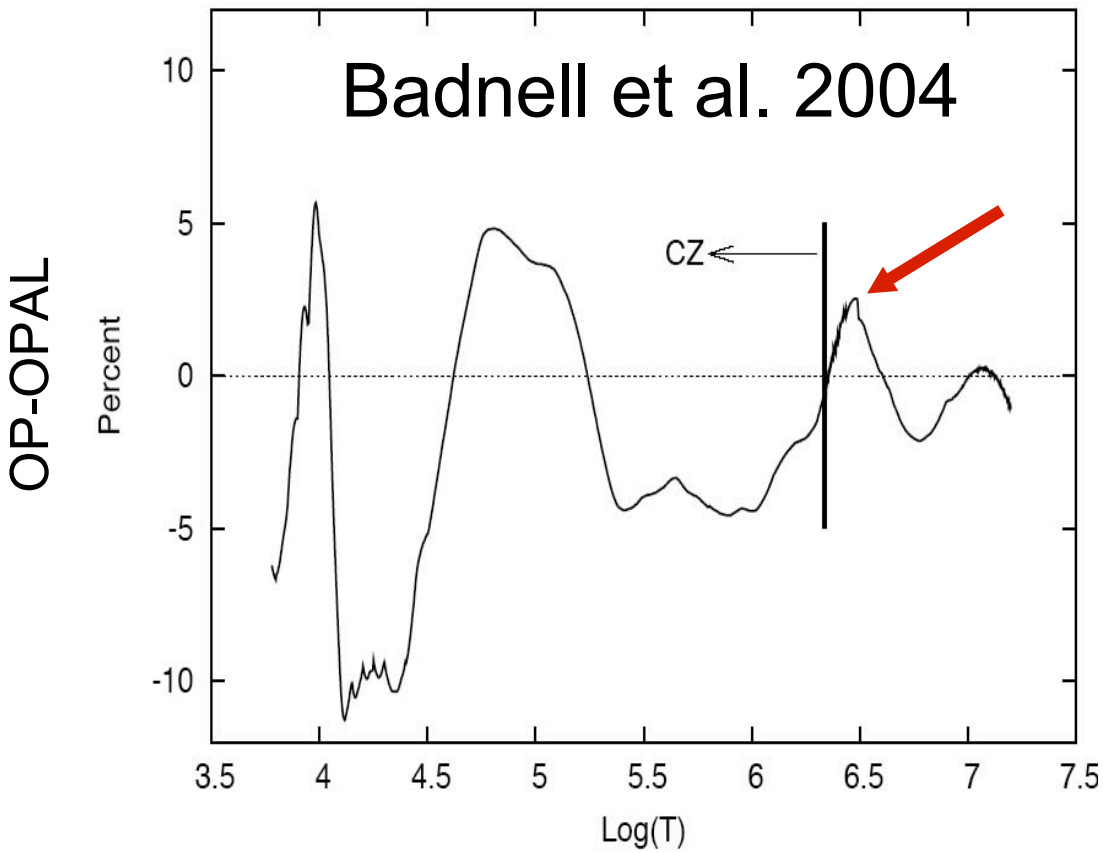

Helioseismic Tests of the New Los Alamos LEDCOP Opacities, 2001,ApJ,561,450

Abstract

We compare the helioseismic properties of two solar models, one calibrated with the OPAL opacities and the other with the recent Los Alamos LEDCOP (Light Element Detailed Configuration Opacity) opacities. We show that, in the radiative interior of the Sun, the small differences between the two sets of opacities (up to 6% near the base of the convection zone) lead to noticeable differences in the solar structure (up to 0.3% in sound speed), with the OPAL model being the closest to the helioseismic data. More than half of the difference between the two opacity sets results from the interpolation scheme and from the relatively widely spaced temperature grids used in the tables. The remaining 3% intrinsic difference between the OPAL and the LEDCOP opacities in the radiative interior of the Sun is well within the error bars on the opacity calculations resulting from the uncertainties on the physics. We conclude that both the OPAL and LEDCOP opacities produce solar models in close agreement with helioseismic inferences, but discrepancies still persist at the level of 0.6% between the calculated and inferred sound speed in the radiative interior of the Sun.

Neuforge-Verheecke, C; Guzik, J.A.; Keady, J.J.; Magee, N.H.; Bradley, P.A.; Noels, A.

Opacity Differences OPAL-LEDCOP versus Solar Model Radius Neuforge-Verheecke, C, et al.,2001

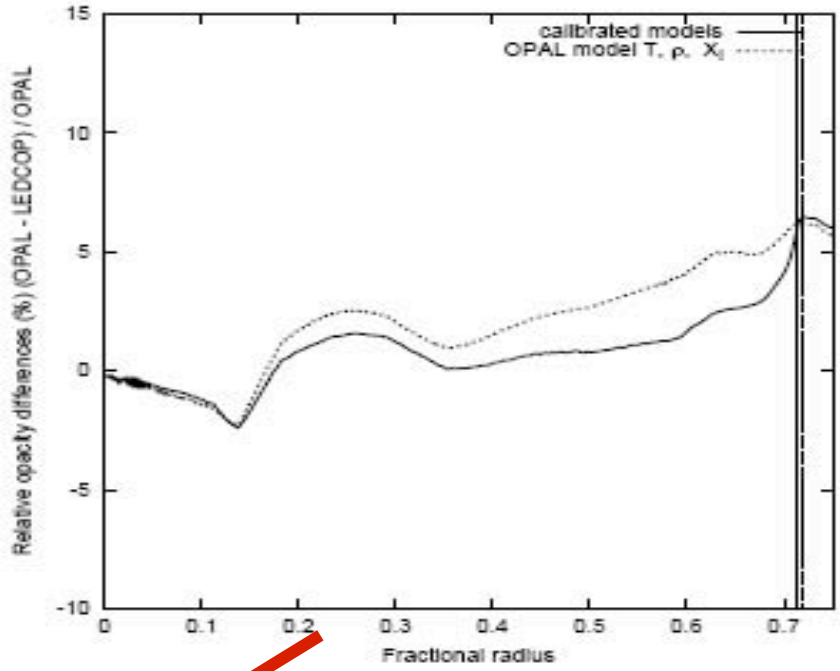

FIG. 1.—Relative opacity differences between the calibrated LEDCOP and OPAL model (*solid line*), and relative differences between the LEDCOP and OPAL opacities calculated with the temperature, density, and composition profile of the OPAL model (*dotted line*), as a function of the fractional radius. The opacity differences that we obtain are very similar in both cases. The first way to compare the OPAL and the LEDCOP opacities, i.e., for the actual run of the physical quantities in the different calibrated models, allows us to link the sound speed differences to the opacity differences, since, in each model, the sound speed is calculated for the actual run of the physical quantities. The vertical lines indicate the convection zone base location in the different models.

β Cephei Model Opacity Temperature Derivative versus Lagrange Mass Shell

Cox. Morgan, Rogers & Iglesias, ApJ, 1992

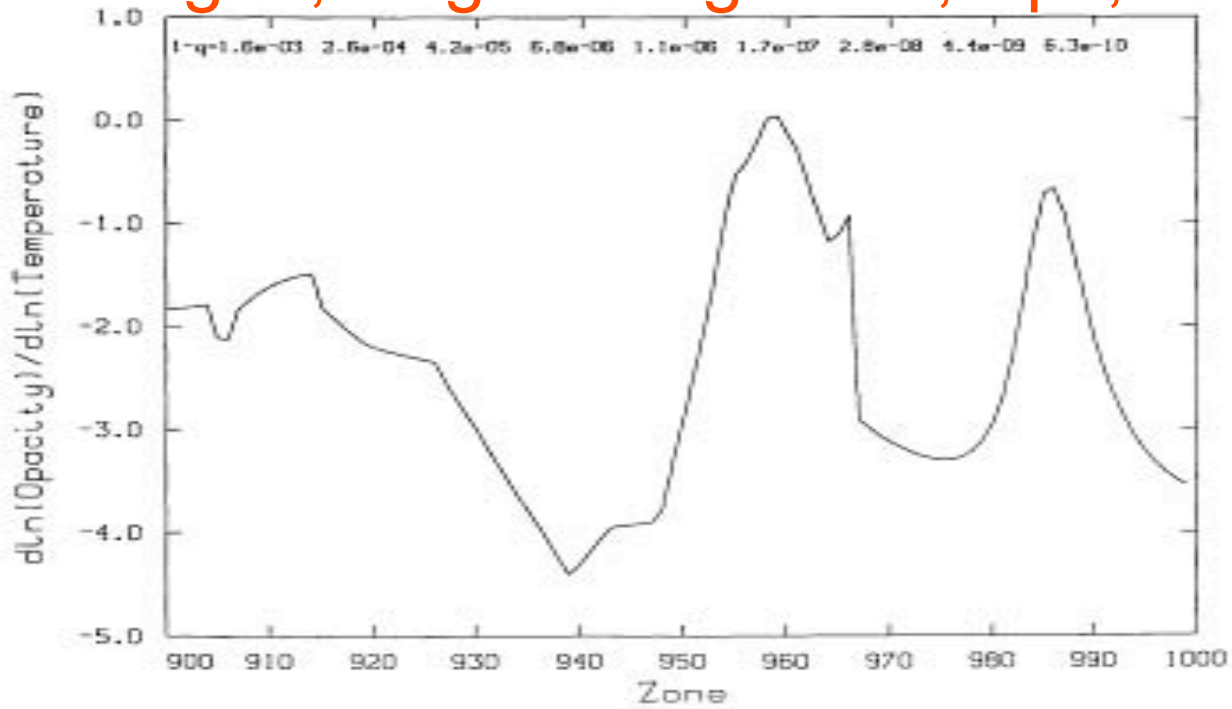

FIG. 1.—The logarithmic derivative of the opacity with respect to temperature vs. zone number is plotted, based on data from Table 1. The surface mass depth for this irregular zoning is indicated at the top. The iron line peak between zones 950 and 970 is in the pulsation driving region. The usual helium ionization region, centered at ~40,000 K lies between zones 980 and 990.

β Cephei Model Pulsational Driving versus Lagrange Mass Shell

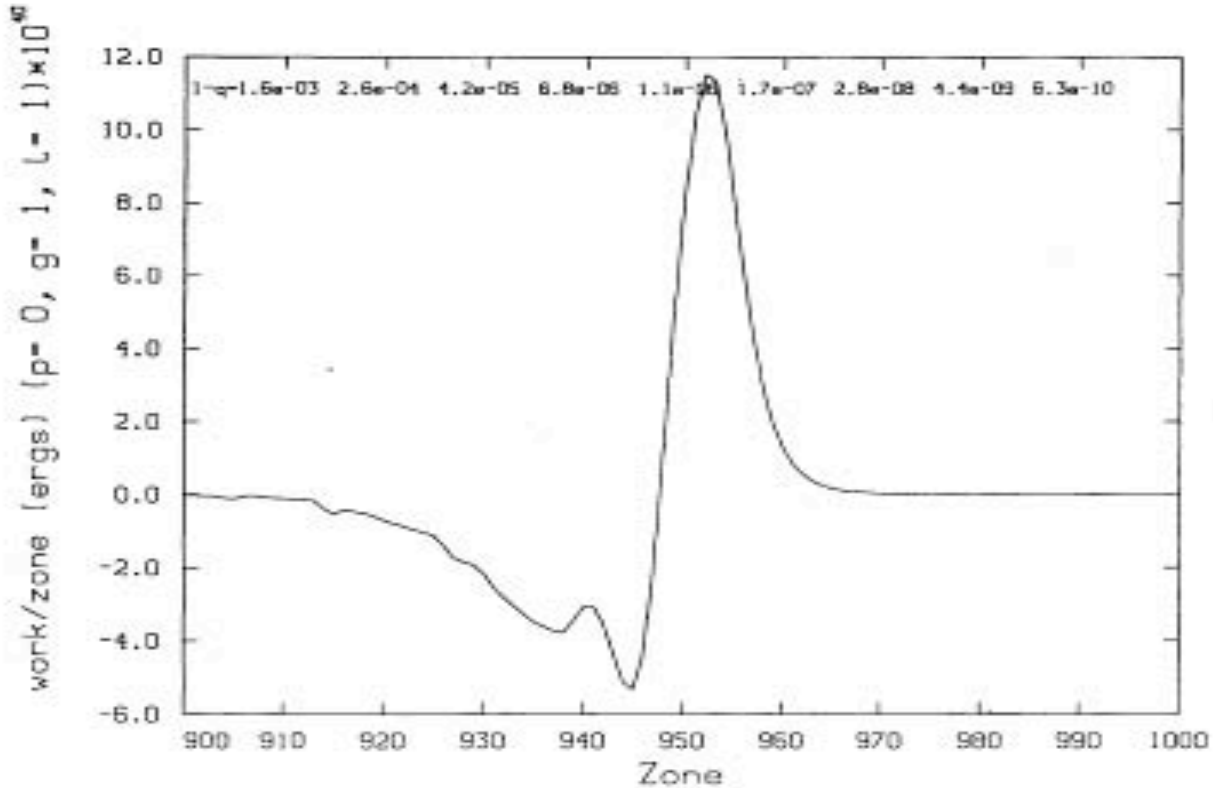

FIG. 2.—The work per zone to drive or damp pulsations is given versus zone number. All the pulsation driving seen is done in the outer 2×10^{-6} of the model mass between temperatures of 100,000 and 250,000 K. The surface mass depth for this irregular zoning is indicated at the top.

Double-Mode RR Lyrae Variable Period Ratios versus Period using OPAL Opacities

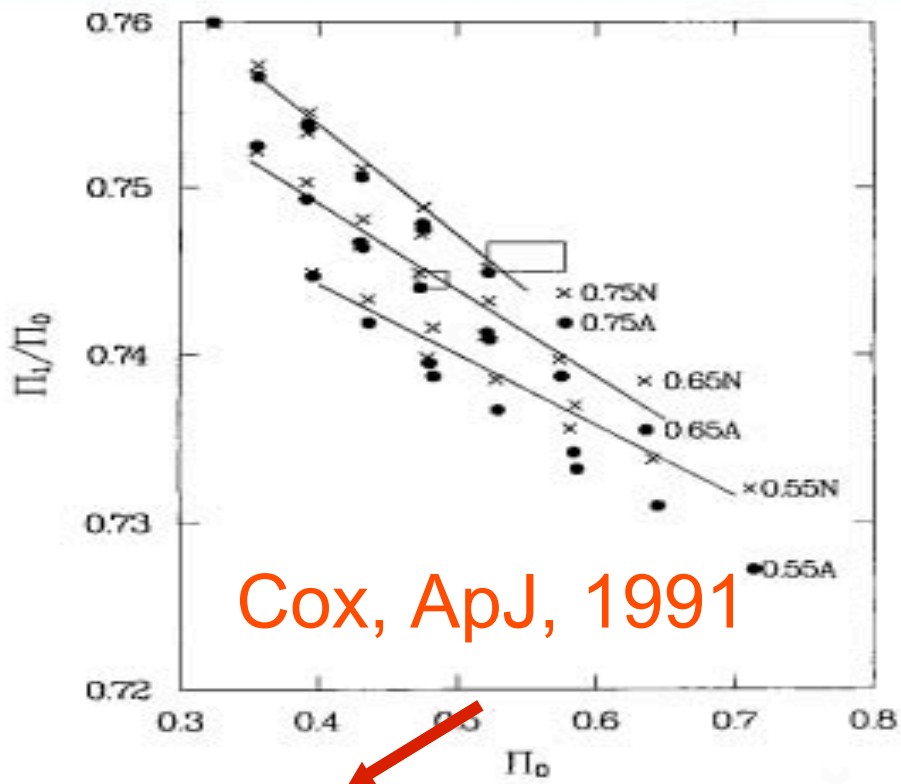

FIG. 1.—Both adiabatic and nonadiabatic period ratios are plotted vs. the fundamental mode periods for the 27 models. A least squares line is plotted for the 0.55, 0.65, and 0.75 $M_\odot$ nonadiabatic cases. The slopes for these lines are −0.0420, −0.0517, and −0.0565 day^{-1}, and the period ratios at 0.5 day are 0.7400, 0.7438, and 0.7471. The left box encloses the Oosterhoff type I cluster variables, whereas the larger box encloses the Oosterhoff type II cluster variables.

Opacity versus Radius for an RR Lyrae Variable Model at the Evolution Mass

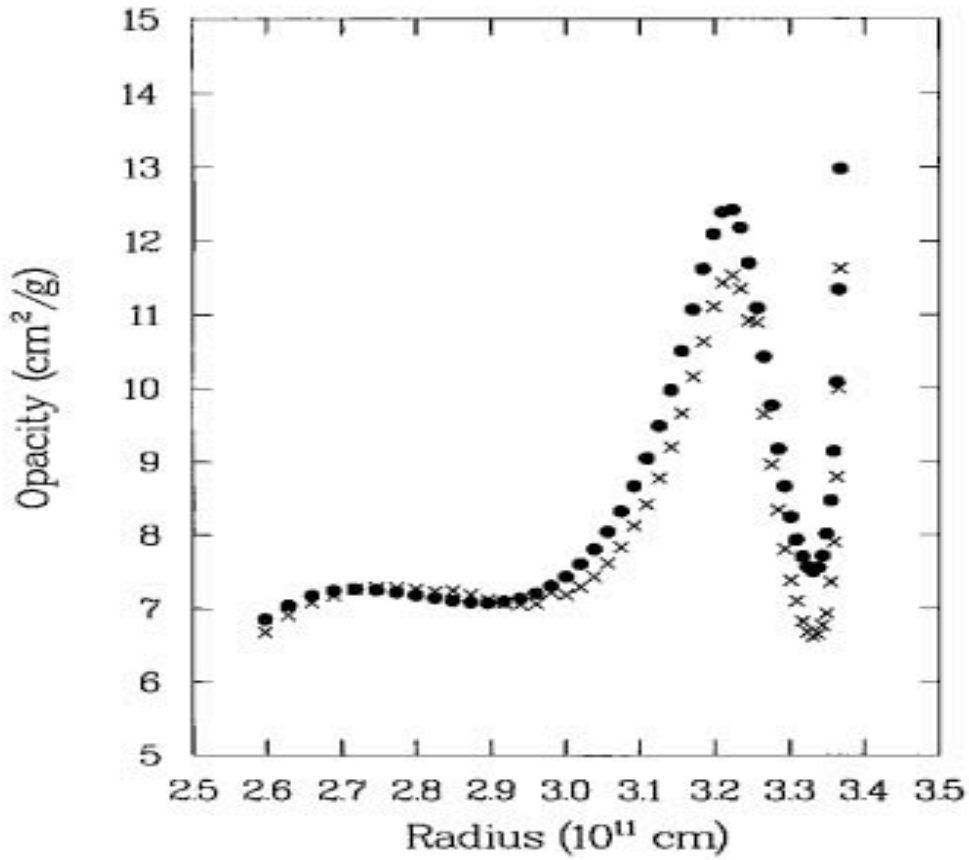

FIG. 2.—Opacity in the two models at 0.65 $M_\odot$ is plotted vs. radius. The reduced opacity model is represented by crosses (×).

δ Scuti and Cepheid Instability Strip Blue Edges for Different Masses and Helium Abundance

Cox, King, & Tabor, ApJ, 1973

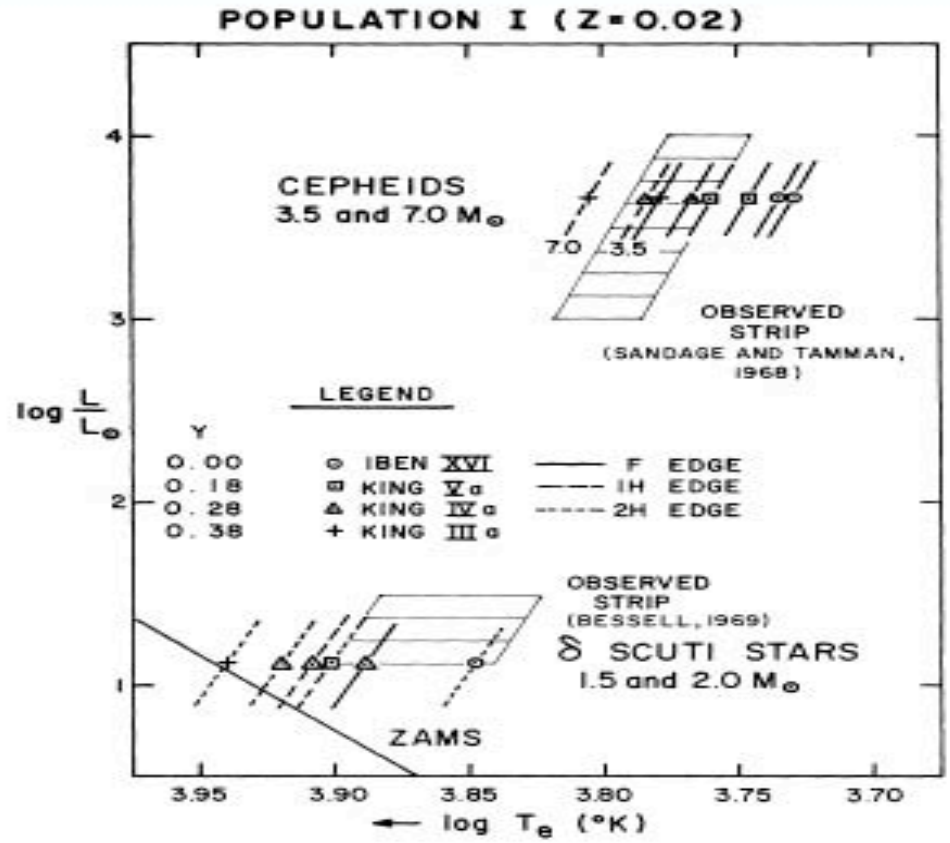

FIG. 5.—Theoretical blue edges for δ Scuti stars and Cepheids in the H-R diagram

Iron Abundance versus Mass Depth for 8 Effective Surface Temperatures for sdB Stellar Models

Charpinet, et al. ApJ, 1997

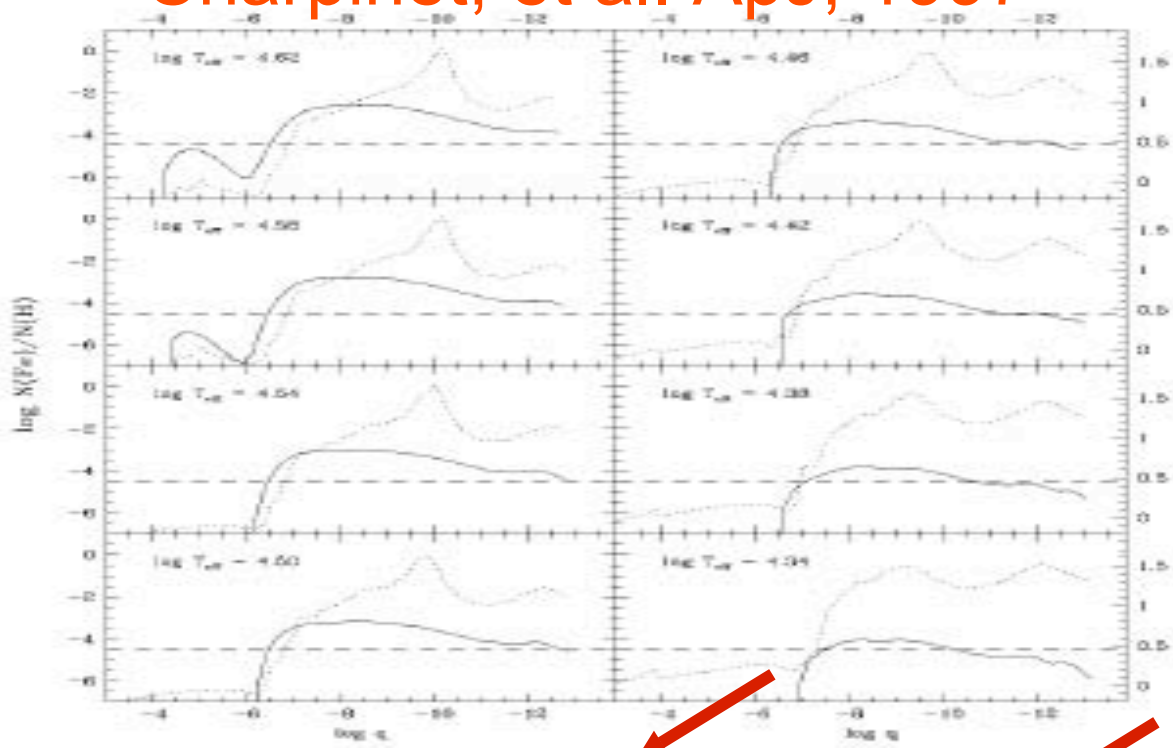

FIG. 1.—Equilibrium abundance of iron (*solid curve*) as a function of the fractional mass depth $\log q$ [$= \log(1 - M(r)/M_*)$] for a series of representative models of sdB stars with $M_* = 0.48\ M_\odot$, $\log g = 5.8$, and $\log T_{eff}$ from 4.34 to 4.62 in steps of 0.04. In each panel the tip of the solid curve on the right hand side corresponds to the location of the Rosseland photosphere. The dashed horizontal line gives the normal value of the Fe/H number ratio. Also shown is the profile of the Rosseland opacity (*dotted curve*); its logarithmic value can be read on the right axis.

Solar Model Observed minus Calculated p-mode Oscillation Frequencies for High Degree

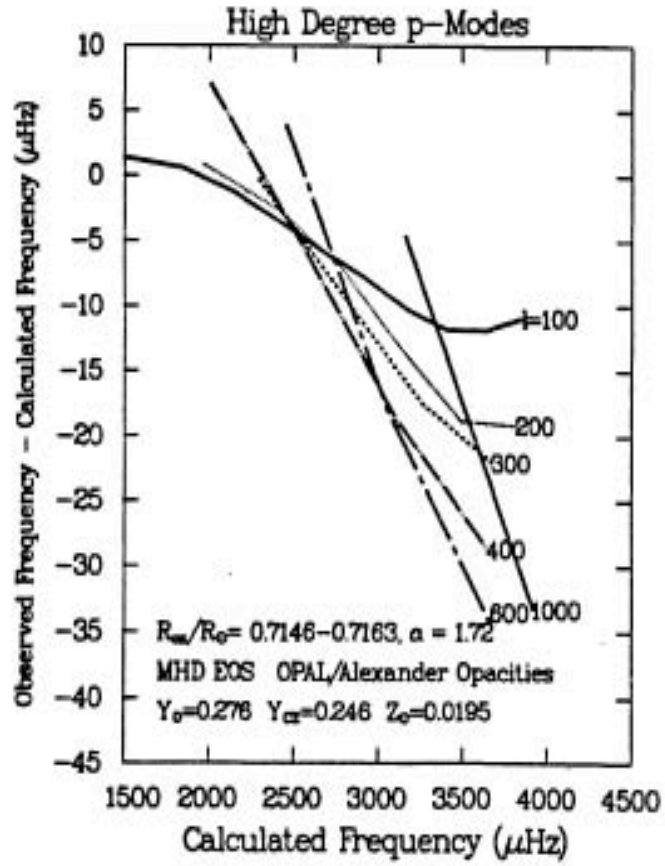

Figure 3. O-C vs. calculated p-mode frequencies of degree $\ell = 100, 200, 300, 400, 600$, and 1000 for MHD EOS solar model described in Fig. 1. Lines connect modes of same degree ℓ and different radial order n. Observations are from Libbrecht et al. (1990).

Solar Model Observed minus Calculated p-mode Oscillation Frequencies for 50% Opacity Increase

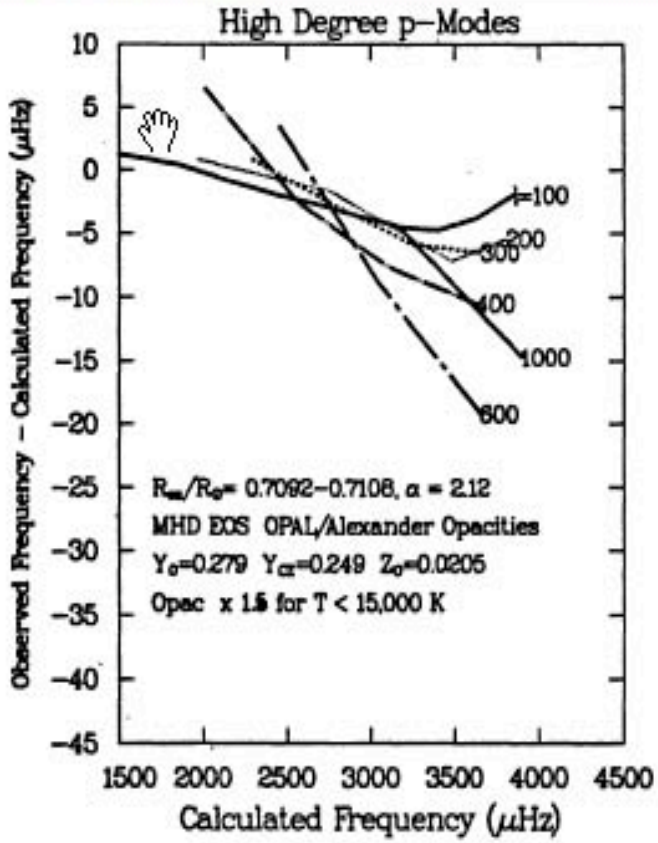

Figure 6: O-C vs. calculated p-mode frequencies of degree $\ell = 100, 200, 300, 400, 600$, and 1000 for MHD EOS model with 50% opacity increase for temperatures < 15,000 K. The opacity increase improves the agreement with observation for these high-degree modes (compare with Fig. 3).

Solar Model Observed minus Calculated p-mode Oscillation Frequencies for 50% Opacity Increase and Turbulent Pressure

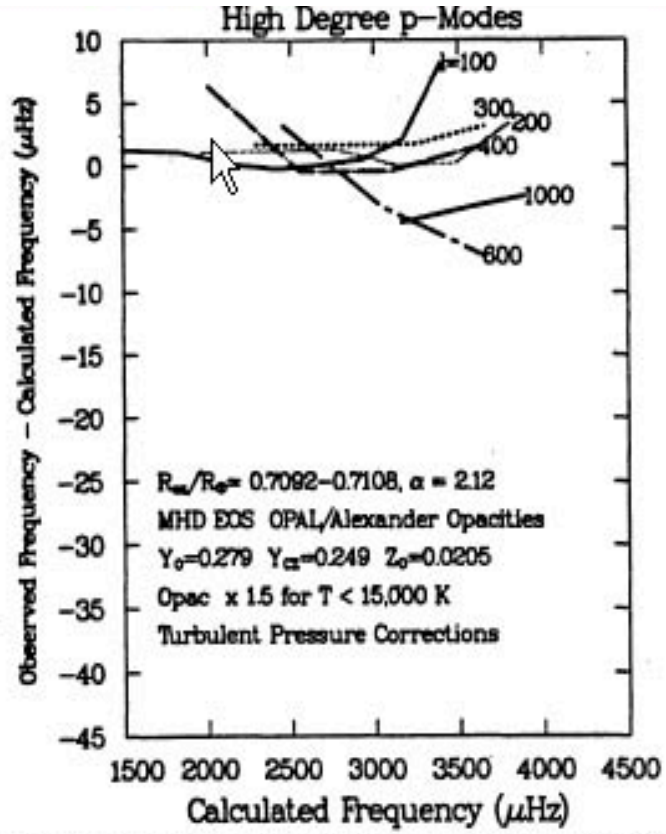

Figure 7. O-C vs. calculated p-mode frequencies of degree $\ell = 100, 200, 300, 400, 600$, and 1000 for MHD EOS model with 50% opacity increase for temperatures $< 15{,}000$ K, and including frequency corrections due to turbulent pressure as calculated by Guzik & Cox (1992). Turbulent pressure further improves agreement with observation for these high-degree modes.

Settling and Radiative Levitation of Solar Elements Using OPAL Monochromatic Data

Turcotte, Richer, Michaud, Igelesias, Rogers, ApJ, 1998

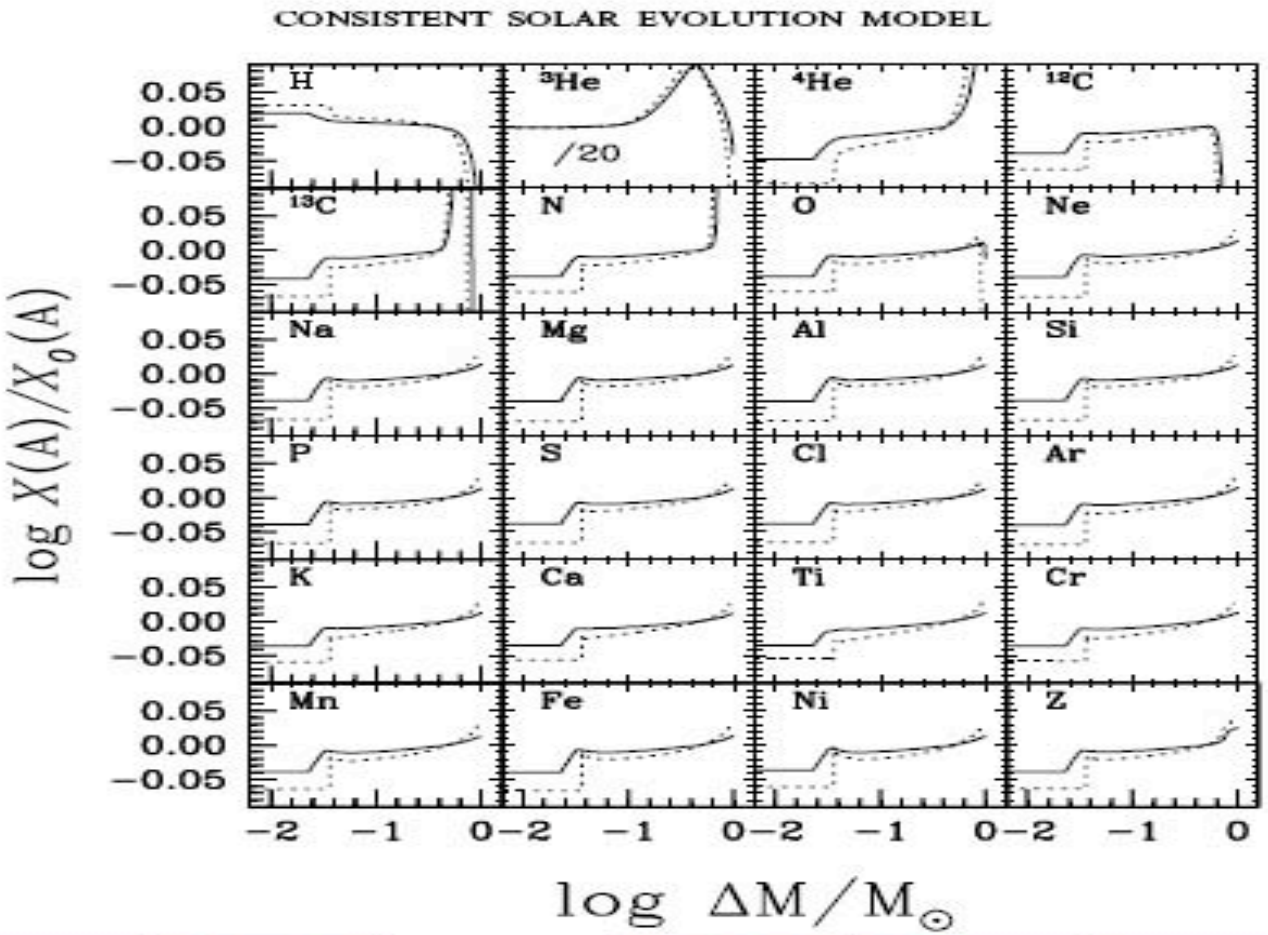

Surface Mass Fraction Composition of GW Virginis Model observed XHe=0.33, XC=0.50, XO=0.17

XH = 0.02057
XHe = 0.43601
XC = 0.16904
XN = 0.000000000
XO = 0.040694
XNe = 0.021265
XNa = 0.00018440
XMg = 0.0033876
XAl = 0.000016262
XSi = 0.00014687

XP = 0.00004010
XS = 0.000051357
XCl = 0.0000043391
XAr = 0.000010271
XCa = 0.0000035543
XTi = 0.00000000000
XCr = 0.0000013147
XMn = 0.00000020743
XFe = 0.000073255
XNi = 0.000036881

On the other hand, my responsibility to society makes me want to stop right here.

"On the other hand, my responsibility to society makes me want to stop right here."